Spin-Wave Theory for the Long-Range Quantum XXZ Model

Sabrina Chern
Department of Physics, Harvard University, Cambridge, MA 02138, USA
(Dated: May 19, 2023)

The rich physics and increasing experimental relevance of long-range interacting spin systems motivates an analytical understanding of their low-energy properties. Using spin wave theory, we study the dispersion relations of the long-range ferromagnetic XXZ model and calculate its anomalous behavior for certain ranges of power-law interactions. We note the generalized Higgs mechanism and its applicability to both ferromagnetic and antiferromagnetic models, and end by commenting on the implications of anomalous behavior for finite temperature order in $d = 2$.

I. INTRODUCTION

Long-range interacting models can have drastically different behavior from their short-range, well-studied counterparts. In the case of classical continuous spins with a $1/r^{d+\sigma}$ interaction, this is manifest in the modifications of the lower and upper critical dimensions to σ and 2σ, respectively. The lower dimension modification is seen through Fourier transforming the long-range term and observing the dimension at which the Goldstone mode fluctuations diverge, and the upper dimension modification through the quartic term in the Landau-Ginzburg theory becomes relevant under RG analysis.[1]

Studies of quantum long-range systems have become simultaneously increasingly studied and experimentally relevant. The physics of long-range interactions can lead to a host of exotic physics at finite and zero temperatures, such as supersolids[2], spin liquids[3], and Haldane phases[4], and can also be relevant for metrology.[5] A variety of modern AMO platforms that can naturally simulate and probe a variety of interesting physics with single-site resolution have long-range interactions, including Rydberg atoms[6], dipolar quantum gases[7], molecules[8], and trapped ions[9]. Many recent studies have strived to understand the critical and ground state properties of these phases. In addition, the low-energy excitations can also tell us about thermodynamic properties.

In this report, we analyze the low-energy excitation spectra of the quantum long-range XXZ model. First, we briefly discuss the short-range model and their Goldstone modes. Then, we consider the mean-field phases of the long-range model, and construct the excitation dispersions above the ground state through a semiclassical spin-wave analysis. We comment on the scaling of the dispersion relations at small momenta, and how long-range interactions can give rise to a generalized Higgs mechanism.[10,11] Finally, we use spin-wave analysis to calculate the critical temperature of the model and compare to results recently reported from quantum Monte Carlo simulations.[12]

II. MODEL

Our model is the $S = \frac{1}{2}$ long-range XXZ model where $J_\perp/J_z$ characterizes the easy-plane anisotropy and α the power law decay:

$$H_{XXZ} = \sum_{ij} \frac{1}{r_{ij}^\alpha}(J_\perp(S_x^i S_x^j + S_y^i S_y^j) + J_z S_z^i S_z^j) \quad (1)$$

We set the magnitude of $J_\perp = -1$ (ferromagnetic interactions), and recover the XY model at $J_z = 0$ and the SU(2)-symmetric Heisenberg model at $J_z = -1$.

A. Short-range Interactions

Let us first begin by reviewing short-range systems with continuous symmetries. Hamiltonians of this family exhibit Goldstone modes, which are collective low-energy excitations that are slowly varying rotations in space.[1] In the context of magnetism, these excitations are often called *spin waves*. Although in rotationally symmetric classical models we found that the Goldstone modes have energy $\propto q^2$, the quantum cases are somewhat subtle.

The number of Goldstone modes in non-relativistic systems is always upper bounded by the number of broken generators of symmetries.[13,14] It is also the dimension of the full symmetry group G divided by the subgroup H preserved after the symmetry-breaking. For example, in U(1) symmetric Hamiltonians, $G = U(1)$ and $H = \{e\}$ is the trivial subgroup, so the number of broken generators, and thus the maximum number of Goldstone modes, is 1. For SO(3), the ordered state still has SO(2) symmetry, so there are at most 2 Goldstone modes corresponding to 2 broken generators.

Formally, to get the dispersion relations of the Goldstone modes, we find the low-energy effective Lagrangian of the broken generators and then solve the resulting equations of motion.[14] For a system with 2 broken generators and possible modes π_a and π_b, this can be written as

$$\mathcal{L}_{eff} = m_{ab}(\pi_a \partial_t \pi_b - \pi_b \partial_t \pi_a) + g^*_{ab} \partial_t \pi_a \partial_t \pi_b - g_{ab} \boldsymbol{\nabla} \pi_a \cdot \boldsymbol{\nabla} \pi_b \quad (2)$$

Fourier transforming this Lagrangian introduces a power of the frequency w for each time derivative and momentum k for each gradient, so the dominant term in this Lagrangian determines the dispersion relation of the excitations.

However, the number of Goldstone modes can be smaller than the number of broken generators. A canonical example is the nearest neighbor Heisenberg ferromagnet: the broken generators S_x, S_y do not excite independent modes.[13] This comes from the fact that the symmetry-broken state is a maximally polarized state, so only the lowering operator S_- actually excites a mode. Thus, the action of both S_x, S_y are equivalent, so there is only one mode. In the Lagrangian above, this means that the terms $\propto m_{ab}$ are dominant, so the dispersion relation is $w \propto k^2$.

In contrast, for the nearest neighbor Heisenberg antiferromagnet, the symmetry-broken state is not the fully polarized state, so there are two independent Goldstone modes for each broken generator.[14] Thus, the dominant term in the Lagrangian is $\propto g^*_{ab}$ and we get $w^2 \propto k^2 \rightarrow w \propto |k|$ for each mode.

For U(1) symmetries, the Lagrangian can only describe one mode, so the dispersion relation is $w \propto |k|$.[14]

Now let's briefly turn our attention to discrete Ising symmetries. Although discrete symmetries don't exhibit Goldstone modes, we can still ask about the dispersion relation of excitations above the gap. For the short-range ferromagnetic Ising model, this can be seen through a low temperature expansion around the ground state of the ordered phase (the quantum 1D system can order by the mapping to the 2D classical system). The energy of the system is $E_k \propto d + \frac{k^2}{4d} \approx \Delta + k^2$ for a d-dimensional system and gap Δ[15].

III. MEAN FIELD PHASE DIAGRAM

Our model hosts three ordered phases when $J_\perp = -1$: an Ising ferromagnet (I-F), Ising antiferromagnet (I-AF), and XY ferromagnet (XY-F).[11,16] We can immediately see this from the limiting cases of $J_z \rightarrow -\infty$, $J_z \rightarrow +\infty$, and $J_z = 0$, respectively. The I-F phase corresponds to spins uniformly pointing along one direction of the z axis, and the I-AF phase corresponds to a staggered magnetization of spins. The XY-F is a phase of spins that break the z rotational symmetry by uniformly pointing in a direction in the xy plane. The phase boundaries can be determined by finding the critical J_z for which each variational ansatz yields the same energy. The energies for these three ansatzes are:[16]

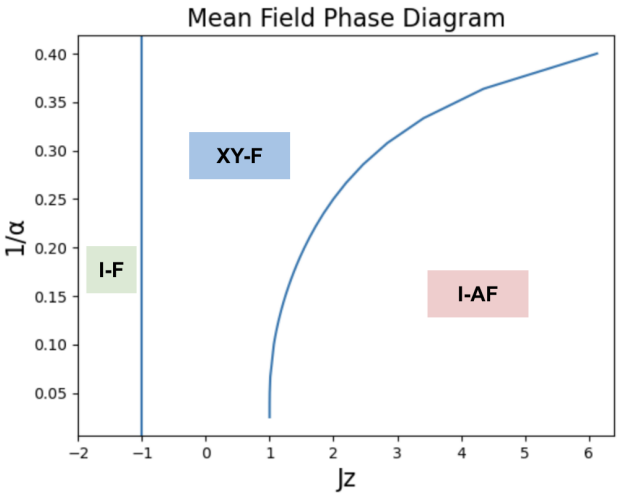

Figure 1: The $d = 2$, $\alpha = 3$ mean-field phase diagram from Equation 6, inspired by Frérot et al[16]. For $J_z < -1$, the system breaks discrete symmetry to order as an Ising ferromagnet. For varying power laws and $J_z > -1$, the ordered phase either is an XY ferromagnet or Ising antiferromagnet. The solid blue lines indicate the mean-field transitions.

$$E_{I-F} = J_z S^2 \sum_{i \neq j} \frac{1}{r_{ij}^\alpha} \tag{3}$$

$$E_{I-AF} = J_z S^2 \sum_{i \neq j} \epsilon_i \epsilon_j \frac{1}{r_{ij}^\alpha} \tag{4}$$

$$E_{XY-F} = -S^2 \sum_{i \neq j} \frac{1}{r_{ij}^\alpha} \tag{5}$$

with $\epsilon_i = 1, -1$ being staggered for each neighboring site. The phase boundary for the I-F is when $J_z < -1$, and we can determine the phase boundary between the XY-F and I-AF by taking $E_{I-AF} = E_{XY-F}$ and solving for $J_{z,crit}$:

$$J_{z,crit}(\alpha) = -\frac{\sum_{i \neq j} \frac{1}{r_{ij}^\alpha}}{\sum_{i \neq j} \epsilon_i \epsilon_j \frac{1}{r_{ij}^\alpha}} \tag{6}$$

Although we will generally discuss arbitrary power-law interactions α in d-dimensions, we will comment in particular about the point $d = 2$, $\alpha = 3$. This is motivated by the recent advances in experimental platforms such as Rydberg atoms, polar molecules, and even solid-state nitrogen vacancy centers[17], which have dipolar interactions. In addition, two-dimensional systems in particular can host exotic phases of matter.[3]

Using the above equation and solving for the critical value numerically yields the mean-field phase diagram in Figure 1.

IV. SPIN WAVE ANALYSIS

In quantum models, we can adopt a semiclassical picture to understand spin waves. We take the spin to approach its classical limit, or $S \gg 1$. The standard method for carrying out this analysis is known as the *Holstein-Primakoff transformation*, which maps spin raising and lowering operators with bosonic creation and annihilation operators. This formalizes the assumption that the state does not greatly deviate from their expectation values, which we assume points along some axis.[18]

We will now consider the dispersion relations of the Ising ferromagnetic and the XY ferromagnetic phases.

A. Spin Wave Theory for the Ising Ferromagnet

First, we will consider the Ising ferromagnetic phase, so we take the mean-field expectation value to lie along the z axis. The mappings, which preserve the commutation relations between the spin operators, are as follows:

$$S_i^z = S - a_i^\dagger a_i \tag{7}$$

$$\begin{aligned} S_i^- &= a_i^\dagger (2S - a_i^\dagger a_i)^{\frac{1}{2}} \\ &= a_i^\dagger \sqrt{2S}(1 - \frac{1}{4S} a_i^\dagger a_i) + \mathcal{O}\left(\frac{1}{S}\right) \end{aligned} \tag{8}$$

$$\begin{aligned} S_i^+ &= (2S - a_i^\dagger a_i)^{\frac{1}{2}} a_i \\ &= \sqrt{2S}(1 - \frac{1}{4S} a_i^\dagger a_i) a_i + \mathcal{O}\left(\frac{1}{S}\right) \end{aligned} \tag{9}$$

Applying this transformation to 1 and keeping terms up to order $1/\mathcal{S}$, we get

$$\begin{aligned} H &= H_0 + H_2 + H_4 + \mathcal{O}\left(\frac{1}{\mathcal{S}}\right) \\ &= \sum_{ij} \frac{1}{r_{ij}^\alpha} \Big\{ J_z S^2 + S(a_i a_j^\dagger + a_i^\dagger a_j) - J_z S(a_j^\dagger a_j + a_i^\dagger a_i) \\ &- (a_i a_j^\dagger a_j^\dagger a_j + a_i^\dagger a_i a_i a_j^\dagger + a_i^\dagger a_i^\dagger a_i a_j + a_i^\dagger a_j^\dagger a_j a_j) \\ &+ J_z a_i^\dagger a_i a_j^\dagger a_j) + \mathcal{O}\left(\frac{1}{\mathcal{S}}\right) \Big\} \end{aligned} \tag{10}$$

We observe that the first-order term H_0 is simply a constant, and H_2 is a quadratic Hamiltonian that describes noninteracting bosons, or the noninteracting Goldstone modes around the expectation value. H_4 describes the interaction between those modes, but for now we truncate up to $\mathcal{O}(\mathcal{S}^0)$ and diagonalize the Hamiltonian by Fourier transforming the bosons by $a_j = \frac{1}{\sqrt{N}} \sum_k e^{-i\vec{k}\cdot\vec{r_j}} a_k$. Then, switching variables to index spin i and the distance between each spin $\vec{r}$ (with a factor of 2 to avoid double-counting), the quadratic Hamiltonian H_2 becomes:

$$\begin{aligned} H_2 &= \frac{1}{2} \sum_{\vec{r_i},\vec{r}} \frac{1}{|r|^\alpha} \left\{ a_i^\dagger a_{i+r} + a_{i+r}^\dagger a_i - J_z(a_i^\dagger a_i + a_{i+r}^\dagger a_{i+r}) \right\} \\ &= \frac{1}{2} \sum_{\vec{r_i},\vec{r}} \frac{1}{|\vec{r}|^\alpha} \Big\{ \frac{1}{N} \sum_{k,k'} e^{i(\vec{k}-\vec{k'})\cdot\vec{r_i}} e^{i\vec{k'}\cdot\vec{r}} a_k^\dagger a_{k'} \\ &+ a_{k'}^\dagger a_k e^{i(\vec{k}-\vec{k'})\cdot\vec{r_i}} e^{-i\vec{k'}\cdot\vec{r}} \\ &- \frac{J_z}{N} \sum_{k,k'} e^{i(\vec{k}-\vec{k'})\cdot\vec{r_i}} a_k^\dagger a_{k'} + a_{k'}^\dagger a_k e^{i(\vec{k}-\vec{k'})\cdot(\vec{r_i}+\vec{r})} \Big\} \\ &= \sum_{k,\vec{r}} \frac{1}{|\vec{r}|^\alpha} (\cos\left(\vec{k}\cdot\vec{r}\right) - J_z) a_k^\dagger a_k \end{aligned} \tag{11}$$

Our Hamiltonian is diagonal in the $a_k, a_k^\dagger$ basis, so we can immediately read out our dispersion relation as the eigenvalues of each k mode. Defining $\epsilon_k = \sum_{\vec{r}} \frac{1}{|\vec{r}|^\alpha} \cos\left(\vec{k}\cdot\vec{r}\right)$ and $\epsilon_0 = \sum_{\vec{r}} \frac{1}{|\vec{r}|^\alpha}$,

$$w(k) = \sum_{\vec{r}} \frac{1}{|\vec{r}|^\alpha} (\cos\left(\vec{k}\cdot\vec{r}\right) - J_z) = \epsilon_q - J_z \epsilon_0 \tag{12}$$

which agrees with the spin-wave excitation spectrum reported previously.[11] In the $d = 2$, $\alpha = 3$ case, $w \propto -J_z\epsilon_0 + |q|$ for small q. Due to the long-range dipolar interactions, the I-F dipersion relation is linear instead of quadratic in the short-range case. Spin excitations now travel ballistically, and the correlation functions decay algebraically as $1/r^3$ even though the phase is gapped.[11]

B. Spin Wave Theory for the XY ferromagnet

The spin-wave theory for the XY ferromagnet is similar to the Ising case, except that we consider fluctuations around the mean-field state of spins pointing in the x direction, or bosonize with respect to the x-vacuum and consider the fluctuations around it.

We rotate our mapping operators to:

$$\begin{aligned} S_i^x &= S - a_i^\dagger a_i \\ S_i^z &= \frac{S_i^+ - S_i^-}{2i} \\ S_i^y &= \frac{-(S_+ + S_i^-)}{2} \end{aligned} \tag{13}$$

Applying the transformation to the Hamiltonian up to order $\mathcal{O}(\mathcal{S}^0)$:

$$
\begin{aligned}
H &= \sum_{ij} \frac{1}{r_{ij}^{\alpha}} S^2 - S(a_i^\dagger a_i + a_j^\dagger a_j) + \frac{S}{2}(a_i^\dagger a_j^\dagger + a_i^\dagger a_j \\
&+ a_i a_j^\dagger + a_i a_j) - \frac{J_z}{2}(a_i a_j - a_i a_j^\dagger - a_i^\dagger a_j + a_i^\dagger a_j^\dagger) \\
&= \frac{1}{2}\sum_{\vec{r_i},\vec{r}} \frac{1}{r_{ij}^{\alpha}} S^2 + S(-a_{\vec{r_i}}^\dagger a_{\vec{r_i}} - a_{\vec{r_i}+\vec{r}}^\dagger a_{\vec{r_i}+\vec{r}} \\
&+ \frac{1}{2}(a_{\vec{r_i}}^\dagger a_{\vec{r_i}+\vec{r}} + h.c. + a_{\vec{r_i}}^\dagger a_{\vec{r_i}+\vec{r}}^\dagger + h.c.)) \\
&+ \frac{SJ_z}{2}(a_{\vec{r_i}}^\dagger a_{\vec{r_i}+\vec{r}} + h.c. - a_{\vec{r_i}}^\dagger a_{\vec{r_i}+\vec{r}}^\dagger - h.c.))
\end{aligned} \tag{14}
$$

After Fourier transforming, the quadratic part of the Hamiltonian becomes

$$
\begin{aligned}
H &= S\sum_k (-\epsilon_0 + \frac{1+J_z}{2}\epsilon_k) a_k^\dagger a_k \\
&+ \frac{(1-J_z)}{2}(e^{-i\vec{k}\cdot\vec{r}} a_k^\dagger a_{-k}^\dagger + e^{i\vec{k}\cdot\vec{r}} a_k a_{-k})
\end{aligned} \tag{15}
$$

and diagonalizing this with a Bogoliubov transformation yields the Hamiltonian with $\xi_k = u_k a_k + v_k a_{-k}^\dagger$

$$
H = \sum_k w_k \xi_k^\dagger \xi_k \tag{16}
$$

where, using the definitions as before:

$$
w_k = \sqrt{(\epsilon_0 - \epsilon_k)(\epsilon_0 - J_z\epsilon_k)} \tag{17}
$$

Approximating $\epsilon_k \approx \int_1^\infty \frac{1}{|\vec{r}|^\alpha} \cos\left(\vec{k}\cdot\vec{r}\right)$, we can calculate the leading-order behavior of the dispersion relation:

$$
\begin{aligned}
w_k &\propto \begin{cases} \left|\vec{k}\right|^{2x_\gamma} & \text{for } \alpha > d+2 \\ \left|\vec{k}\right|^{(\alpha-d)x_\gamma} & \text{for } d < \alpha < d+2 \end{cases} \\
x_\gamma &= \begin{cases} 1 & \text{for } |J_z| = 1 \\ \frac{1}{2} & \text{for } |J_z| \neq 1 \end{cases}
\end{aligned} \tag{18}
$$

This recovers the short range case that we discussed in Section II A. At the Heisenberg point when $J_z = -1$, $w \propto k^2$, but in the XY phase, we recover the linear dispersion relation $w \propto |k|$.

In our special case of $d = 2$, $\alpha = 3$, the long-range XY-F has Goldstone modes that go as $w_k \propto \sqrt{|k|}$ at small momenta. This is the so-called "anomalous" behavior: although the modes are still gapless, they behave very differently. We can immediately use this relation to support the existence of long-range order at finite temperatures for dipolar interactions. w_k becomes singular as $k \to 0$, so at small temperatures the spin waves are suppressed and order persists at $T > 0$.[12]

V. GENERALIZED HIGGS MECHANISM

Thus far, we have discussed how long-range interactions in the regime $\alpha > d$ can modify the low-energy excitations. However, there are two regions that we could extend our analysis to: very long-range interactions, or $\alpha < d$, and the case of antiferromagnets, or $J_\perp = +1$.

In the first case of $\alpha < d$, the integral ϵ_k diverges in the thermodynamic limit and one needs to perform a regularization, or rescaling time and frequencies. Physically, very long-range interactions cause excitations to propagate increasingly faster for larger system sizes, eventually reaching an unbounded velocity. Rescaling allows us to get a finite dispersion relation in the thermodynamic limit.[10]

Although we will not go into detailed calculations here, performing this regularization leads to a gapped spectrum in the thermodynamic limit, i.e. the Goldstone modes in the XY-F phase become gapped. This is the motivation behind the name of the generalized Higgs mechanism: just as gauge fields acquire a "mass" by coupling to an order parameter, long-range interactions can mediate this coupling and provide a mass for the Goldstone mode.[1,10]

In the second case of XY antiferromagnets, spin-wave theory predicts a slightly different dispersion relation:[10,11]

$$
w_k \propto \begin{cases} \left|\vec{k}\right| & \text{for } \alpha > d+2 \\ \left|\vec{k}\right|^{\frac{2+\alpha-d}{2}} & \text{for } d-2 < \alpha < d+2 \end{cases} \tag{19}
$$

In the short-range limit, the dispersion relation is linear, which recovers the short-range Heisenberg antiferromagnet case where there are two independent Goldstone modes in Section II A. The exponent does not depend on whether the model has full SU(2) symmetry or not. The integral ϵ_k also diverges at a lower dimension for the antiferromagnetic case because of the oscillatory nature of the interactions.

Putting all of this information together, there are three cases of spin wave behavior: gapless and "standard" Goldstone mode behavior, gapless and "anomalous" behavior, and gapped "Higgs" behavior. Figure 2 summarizes the expected behavior for the ferromagnetic (FM) and antiferromagnetic (AFM) cases.

VI. ESTIMATING THE CRITICAL TEMPERATURE OF THE XY FERROMAGNET

As mentioned at the end of Section IV B, the spin-wave excitations allows us to infer that there is true finite-temperature order in the dipolar XY model in two dimensions.

We can use the XY-F dispersion relation found earlier to estimate the critical temperature of the boson con-

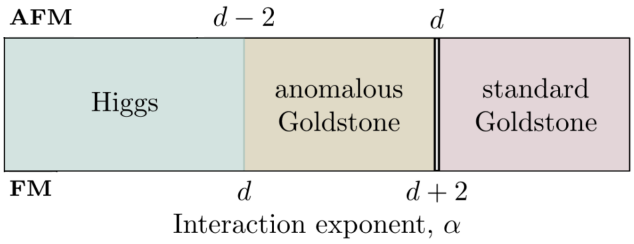

Figure 2: For both the FM and AFM models, $\alpha > d+2$ is sufficiently short-range to recover the standard Goldstone modes. For $d < \alpha < d+2$ for the ferromagnetic case, we get anomalous Goldstone behavior, such as $w \propto \sqrt{k}$ for $d = 2, \alpha = 3$. For the antiferromagnet, this anomalous behavior extends down to $d-2$. For sufficiently long-range interactions in both cases, the Goldstone modes acquire a mass and become gapped.

densation (BEC), or equivalently XY ferromagnetic ordering.

To do this, one should follow the procedure outlined in Nakano and Takahashi, but extend this to two dimensions[5,19]. First, we minimize the free energy of the quadratic Hamiltonian (Equation 16) in the variational manifold of Gaussian states with $n_{\vec{k}}$ bosons in each $\vec{k} = (k_x, k_y)$ mode:

$$|n_{\vec{k}}\rangle = \prod_{\vec{k}} \frac{1}{\sqrt{n_{\vec{k}}!}} (b_{\vec{k}}^\dagger)^{n_{\vec{k}}} |\Psi_{vac}\rangle \tag{20}$$

The key point is that in the sector $M = \sum_k \langle n_k \rangle$, we can use the grand canonical ensemble to allow the BEC to act as a source with average occupation μ. Then, the ordering temperature T_c occurs when $\mu = 0$, or all M particles occupy excited modes. We evaluate the energy in this sector using Wick's theorem:

$$\langle H \rangle = \sum_{|k|} n(\vec{k}) \left(S - \frac{M-1}{2N} \right) \omega_k \tag{21}$$

and get the relation $\frac{\partial E}{\partial k}$, using this to solve the below equation for T_c

$$S = \frac{1}{N} \sum_{\vec{k}} \frac{1}{e^{\beta_c \epsilon(\vec{k})} - 1} \tag{22}$$

The critical temperature is given by the formula

$$T_c = -\frac{S 2^{1-\alpha} \pi^2}{\Gamma[\frac{\alpha}{2}]^2 \sin\frac{\pi\alpha}{2}} \left(\frac{2\pi S(\alpha-2)}{\Gamma[\frac{2}{\alpha-2}]\zeta[\frac{2}{\alpha-2}]} \right)^{\frac{\alpha-2}{2}} \tag{23}$$

which yields $T_c = 2.1708$ for $\alpha = 3$. Recent quantum Monte Carlo simulations reported $T_c = 1.923(1)$.[12] The spin wave theory predicts a higher critical temperature, which could be due to the spin waves absorbing little entropy at low temperatures $S \propto T^4$.[12]

VII. CONCLUSIONS

In this report, we investigated the low-energy properties of the long-range ferromagnetic XXZ model. First, we discussed the expected short-range behavior, which was subtle for the ferromagnetic Heisenberg case. Then, we calculated the mean-field phase diagram of the model, as well as the spin-wave theory for the I-F and XY-F phases. This calculation allowed us to observe a range of power-law decays that gave rise to "anomalous" Goldstone modes, which can drastically change the thermodynamic behavior of the phase. One immediately obvious conclusion in $d = 2$, $\alpha = 3$ is the existence of finite-temperature order.

In addition, although we did not discuss the calculations, a similar analysis can be done for antiferromagnetic models. Taken together, we can observe that the Goldstone modes acquire a mass (become gapped) for $\alpha < d$ in the FM and $\alpha < d-2$ in the AFM.

Spin wave theory offers an extremely useful analytical understanding of the low-energy physics in long-range systems. The development of highly controllable quantum simulators offers an exciting path for probing these dispersion relations in the future.

Acknowledgments. The author thanks M. Kardar and Changnan Peng for a great semester, as well as Maxwell Block and Phil Crowley for discussions on the expected dispersion relations for the ferro vs. anti-ferro short-range Heisenberg and short vs. long-range Ising models. Finally, the author thanks Justin Phillips for proofreading the manuscript.

[1] M. Kardar, *Statistical Physics of Fields* (Cambridge University Press, 2013).

[2] L. Pollet, J. D. Picon, H. P. Büchler, and M. Troyer, "Supersolid phase with cold polar molecules on a triangular lattice," Phys. Rev. Lett. **104**, 125302 (2010).

[3] N. Y. Yao, M. P. Zaletel, D. M. Stamper-Kurn, and A. Vishwanath, "A quantum dipolar spin liquid," Nature Physics **14**, 405–410 (2018).

[4] E. G. Dalla Torre, E. Berg, and E. Altman, "Hidden order in 1d bose insulators," Phys. Rev. Lett. **97**, 260401 (2006).

[5] M. Block, B. Ye, B. Roberts, S. Chern, W. Wu, Z. Wang, L. Pollet, E. J. Davis, B. I. Halperin, and N. Y. Yao, "A universal theory of spin squeezing," (2023), arXiv:2301.09636 [quant-ph] .

[6] A. Browaeys and T. Lahaye, "Many-body physics with individually controlled rydberg atoms," Nature Physics **16**, 132–142 (2020).

[7] A. Griesmaier, J. Werner, S. Hensler, J. Stuhler, and T. Pfau, "Bose-einstein condensation of chromium," Physical Review Letters **94** (2005), 10.1103/physrevlett.94.160401.

[8] K.-K. Ni, S. Ospelkaus, M. H. G. de Miranda, A. Pe'er, B. Neyenhuis, J. J. Zirbel, S. Kotochigova, P. S. Julienne, D. S. Jin, and J. Ye, "A high phase-space-density gas of polar molecules," Science **322**, 231–235 (2008).

[9] C. Monroe, W. Campbell, L.-M. Duan, Z.-X. Gong, A. Gorshkov, P. Hess, R. Islam, K. Kim, N. Linke, G. Pagano, P. Richerme, C. Senko, and N. Yao, "Programmable quantum simulations of spin systems with trapped ions," Reviews of Modern Physics **93** (2021), 10.1103/revmodphys.93.025001.

[10] O. K. Diessel, S. Diehl, N. Defenu, A. Rosch, and A. Chiocchetta, "Generalized higgs mechanism in long-range interacting quantum systems," (2022), arXiv:2208.10487 [cond-mat.quant-gas] .

[11] D. Peter, S. Müller, S. Wessel, and H. P. Büchler, "Anomalous behavior of spin systems with dipolar interactions," Physical Review Letters **109** (2012), 10.1103/physrevlett.109.025303.

[12] B. Sbierski, M. Bintz, S. Chatterjee, M. Schuler, N. Y. Yao, and L. Pollet, "Magnetism in the two-dimensional dipolar xy model," (2023), arXiv:2305.03673 [cond-mat.quant-gas] .

[13] H. Watanabe, "Counting rules of nambu–goldstone modes," Annual Review of Condensed Matter Physics **11**, 169–187 (2020).

[14] A. J. Beekman, L. Rademaker, and J. van Wezel, "An introduction to spontaneous symmetry breaking," SciPost Phys. Lect. Notes , 11 (2019).

[15] S. Sachdev, *Quantum Phase Transitions* (Cambridge University Press, 1999).

[16] I. Frérot, P. Naldesi, and T. Roscilde, "Entanglement and fluctuations in the XXZ model with power-law interactions," Physical Review B **95** (2017), 10.1103/physrevb.95.245111.

[17] E. J. Davis, B. Ye, F. Machado, S. A. Meynell, W. Wu, T. Mittiga, W. Schenken, M. Joos, B. Kobrin, Y. Lyu, Z. Wang, D. Bluvstein, S. Choi, C. Zu, A. C. B. Jayich, and N. Y. Yao, "Probing many-body dynamics in a two-dimensional dipolar spin ensemble," Nature Physics (2023), 10.1038/s41567-023-01944-5.

[18] A. Altland and B. Simons, *Condensed Matter Field Theory* (Cambridge University Press, 2010).

[19] H. Nakano and M. Takahashi, "Quantum heisenberg model with long-range ferromagnetic interactions," Phys. Rev. B **50**, 10331–10334 (1994).

Critical Temperature for the XY Ferromagnet

We expand on the calculation that leads to Equation 23. First, we make the integral approximation to evaluate w_k:

$$\begin{aligned}
\omega(\vec{k}) &= \sum_{|r|=1}^{N-1} \frac{1}{|\vec{r}|^{\alpha}} Re[e^{i\vec{k}\cdot\vec{r}}] \\
&= \sum_{r_x,r_y} \frac{1}{(r_x^2+r_y^2)^{\frac{\alpha}{2}}} (\cos(k_x r_x + k_y r_y)) \\
&\approx \int_1^{\infty} r dr \int_0^{2\pi} d\theta \frac{1}{r^{\alpha}} (cos(krcos\theta)) \\
&= \int_1^{\infty} dr \frac{2\pi}{r^{\alpha-1}} [J_0(kr)] \\
&= 2\pi \left(\frac{2^{-\alpha}\alpha\Gamma\left(-\frac{\alpha}{2}\right) k^{\alpha-2}}{\Gamma\left(\frac{\alpha}{2}\right)} - \frac{{}_1F_2\left(1-\frac{\alpha}{2}; 1, 2-\frac{\alpha}{2}; -\frac{k^2}{4}\right)}{\alpha-2}\right)
\end{aligned}$$

where ${}_1F_2(a;b;c;z)$ is the hypergeometric function.
Expanding in powers of k:

$$\begin{aligned}
&= 2\pi \left(\frac{2^{-\alpha}\alpha\Gamma\left(-\frac{\alpha}{2}\right)}{\Gamma\left(\frac{\alpha}{2}\right)} k^{\alpha-2} + \frac{1}{4(\alpha-4)} k^2 - \frac{1}{64(\alpha-6)} k^4 + ...\right) \\
&= f_1 k^{\alpha-2} + f_2 k^2 + O(k^3), \quad f_2 = \frac{2\pi}{4(\alpha-4)}, \quad f_1 = \frac{2^{1-\alpha}\pi\alpha\Gamma[\frac{-\alpha}{2}]}{\Gamma[\frac{\alpha}{2}]} = -\frac{2^{2-\alpha}\pi^2}{\Gamma[\frac{\alpha}{2}]^2 \sin\frac{\pi\alpha}{2}}
\end{aligned}$$

Now the dispersion relation is

$$\begin{aligned}
\epsilon(k) &\approx J\frac{S}{2}\omega(\vec{k}) \\
&\approx \frac{JS}{2}(f_1 k^{\alpha-2} + f_2 k^2) \\
\frac{\partial\epsilon}{\partial k} &\approx \frac{JS}{2}[(\alpha-2)k^{\alpha-3} f_1 + 2 f_2 k]
\end{aligned}$$

We neglect the k^2 term to invert $\epsilon(k)$:

$$\begin{aligned}
k(\epsilon) &= \frac{2\epsilon}{JSf_1}^{\frac{1}{\alpha-2}} \\
\frac{\partial k}{\partial\epsilon} &= \left(\frac{2}{JSf_1}\right)^{\frac{1}{\alpha-2}} \frac{1}{\alpha-2} \epsilon^{\frac{3-\alpha}{\alpha-2}}
\end{aligned}$$

Now we solve for T_c:

$$
\begin{aligned}
S &= \frac{1}{N}\sum_{\vec{k}} \frac{1}{e^{\beta_c \epsilon(\vec{k})}-1} \\
&\approx \frac{1}{(2\pi)^2}\int_0^{\pi} \frac{2\pi k dk}{e^{\beta_c\epsilon(k)}-1} \\
&= \frac{1}{2\pi}\int_0^{w(\pi)} \frac{dw}{e^w-1}(\frac{2\epsilon}{JSf_1})^{\frac{1}{\alpha-2}}\frac{dk}{dw}, \quad w \equiv \beta_c\epsilon \\
&= \frac{1}{2\pi}\int_0^{w(\pi)} \frac{dw}{e^w-1}(\frac{2wT_c}{JSf_1})^{\frac{1}{\alpha-2}}T_c\frac{dk}{d\epsilon} \\
&= \frac{1}{2\pi}\int_0^{w(\pi)} \frac{dw}{e^w-1}(\frac{2wT_c}{JSf_1})^{\frac{1}{\alpha-2}}T_c(\frac{2}{JSf_1})^{\frac{1}{\alpha-2}}\frac{1}{\alpha-2}(wT_c)^{\frac{3-\alpha}{\alpha-2}} \\
&= \frac{1}{2\pi(\alpha-2)}(\frac{2}{JSf_1})^{\frac{2}{\alpha-2}}\int_0^{w(\pi)} \frac{dw}{e^w-1}T_c^{\frac{2}{\alpha-2}}w^{\frac{4-\alpha}{\alpha-2}} \\
&\approx \frac{1}{2\pi(\alpha-2)}(\frac{2}{JSf_1})^{\frac{2}{\alpha-2}}T_c^{\frac{2}{\alpha-2}}\Gamma[\frac{2}{\alpha-2}]\mathrm{Li}_{\frac{2}{\alpha-2}}(1) \\
&= \frac{1}{2\pi(\alpha-2)}(\frac{2}{JSf_1})^{\frac{2}{\alpha-2}}T_c^{\frac{2}{\alpha-2}}\Gamma[\frac{2}{\alpha-2}]\zeta(\frac{2}{\alpha-2})
\end{aligned}
$$

and inverting this we get a T_c estimate, which we calculate numerically for $\alpha = 3$.

$$
\begin{aligned}
T_c &= \frac{JSf_1}{2}(\frac{2\pi S(\alpha-2)}{\Gamma[\frac{2}{\alpha-2}]\zeta[\frac{2}{\alpha-2}]})^{\frac{\alpha-2}{2}} \\
&= \frac{-JS}{2}\frac{2^{2-\alpha}\pi^2}{\Gamma[\frac{\alpha}{2}]^2\sin\frac{\pi\alpha}{2}}(\frac{2\pi S(\alpha-2)}{\Gamma[\frac{2}{\alpha-2}]\zeta[\frac{2}{\alpha-2}]})^{\frac{\alpha-2}{2}} \\
&= \frac{-JS2^{1-\alpha}\pi^2}{\Gamma[\frac{\alpha}{2}]^2\sin\frac{\pi\alpha}{2}}\left(\frac{2\pi S(\alpha-2)}{\Gamma[\frac{2}{\alpha-2}]\zeta[\frac{2}{\alpha-2}]}\right)^{\frac{\alpha-2}{2}}
\end{aligned}
$$